

Invariant Curves and Explosion of Periodic Islands in Systems of Piecewise Rotations*

Peter Ashwin[†] and Arek Goetz[‡]

Abstract. Invertible piecewise isometric maps (PWIs) of the plane, in spite of their apparent simplicity, can show a remarkable number of dynamical features analogous to those found in nonlinear smooth area preserving maps. There is a natural partition of the phase space into an exceptional set, $\bar{\mathcal{E}}$, consisting of the closure of the set of points whose orbits accumulate on discontinuities of the map, and its complement.

In this paper we examine a family of noninvertible PWIs on the plane that consist of rotations on each of four atoms, each of which is a quadrant. We show that this family gives examples of global attractors with a variety of geometric structures. On some of these attractors, there appear to be nonsmooth invariant curves within $\bar{\mathcal{E}}$ that form barriers to ergodicity of any invariant measure supported on $\bar{\mathcal{E}}$. These invariant curves are observed to appear on perturbations of an “integrable” case where the exceptional set is a union of annuli and it decomposes into a one-dimensional family of interval exchange maps that may be minimal but nonergodic. We have no adequate theoretical explanation for the curves in the nonsmooth case, but they appear to come into existence at the same times as an explosion of periodic islands near where the interval exchanges used to be located. We exhibit another example—a piecewise rotation on the plane with two atoms that also appears to have nonsmooth invariant curves.

Key words. planar piecewise isometry, nonuniquely ergodic interval exchange

AMS subject classifications. 37B10, 37E15, 20C20, 68W30

DOI. 10.1137/040605394

1. Introduction. Piecewise isometries are natural generalizations of interval exchange transformations (IETs) and interval translation maps and are of current interest because they arise in a number of applications. These include signal processing [13], rounding and discretization effects [30], Hamiltonian systems [27, 28], and printing processes [2]. Roughly speaking, a piecewise isometry is a map that is simply an isometry on each of a number of disjoint domains. More precisely, suppose that $T : M \rightarrow M$ is an invertible map of a region $M \subset \mathbb{C}$ to itself such that for some partition of M into open disjoint polygons P_i , T is an orientation preserving isometry on each P_i . In such cases we say T is a *piecewise isometry map* (PWI).

If we consider the zero measure set given by the union \mathcal{E} of all preimages of the set of discontinuities D , then its closure $\bar{\mathcal{E}}$ (which may be of positive measure) is referred to as the

*Received by the editors March 18, 2004; accepted for publication (in revised form) by T. Sauer September 22, 2004; published electronically April 22, 2005.

<http://www.siam.org/journals/siads/4-2/60539.html>

[†]Department of Mathematical Sciences, University of Exeter, Exeter EX4 4QE, UK (p.ashwin@ex.ac.uk). The work of this author was partially supported by a Leverhulme Research Fellowship.

[‡]Department of Mathematics, 1600 Holloway Avenue, San Francisco State University, San Francisco CA 94132 (goetz@sfsu.edu). The work of this author was partially supported by an LMS visitor grant, by the NSF research grants DMS 0103882 and OIP 0202732, and in Spring 2002 by San Francisco State Presidential Research Leave.

exceptional set for the map. The complement of the exceptional set is called the *regular set* for the map and consists of disjoint polygons or disks that are periodically coded by their itinerary through the atoms of the PWI. In the case that T is noninvertible, there may exist a global attractor. We say there is a global attractor \tilde{M} if this bounded set is the union of accumulation points of all forward trajectories. Note that \tilde{M} need not be a finite-sided polygon even if all the P_i are such.

It is difficult to show the existence of and to characterize all but the simplest global attractors for piecewise isometries. One of the aims of this paper is to highlight some interesting dynamical and geometric examples of global attractors in the hope that this will contribute to an understanding of the richness of the general case.

We do this by introducing a family of examples of piecewise isometries with four convex (unbounded) atoms that are the standard quadrants of the complex plane. For this family of maps we find numerical evidence of a number of interesting effects. We have found examples of global attractors with many different connected components (possibly a countably infinite number) and with a range of different geometric forms of boundary—for example, polygons, circles, regions with a mixture of straight and curved boundaries, smooth and possibly non-smooth curves, and multiply connected regions.

We consider a special family of “integrable” examples where the exceptional set $\bar{\mathcal{E}}$ has an open interior but is nonergodic. On this $\bar{\mathcal{E}}$ the dynamics reduces to a family of nontrivial IETs on a union of one-dimensional curves. The dynamics on these curves may be minimal but nonuniquely ergodic. We observe the following:

- For general perturbations, the family of exchanges breaks up to form a large number of periodic islands.
- For a specific family of perturbations, there appear to be invariant curves within $\bar{\mathcal{E}}$ that are Lipschitz, but not differentiable, embeddings of curves. We refer to these as *nonsmooth invariant curves*.
- The nonsmooth invariant curves appear to come in discrete families and appear to be limits of sequences of periodic disks.
- The global attractor in the “integrable” case is a union of two disks up to a set of zero measure (see Theorem 4.5).
- For small perturbations from the “integrable” case, the global attractor becomes much more complicated. For general perturbations, the global attractor appears to become a totally disconnected union of disks, whereas more complicated connected components appear in cases where there are nonsmooth invariant curves in the exceptional set.

This break-up of an “integrable” case with smooth invariant curves to a union of periodic islands and invariant curves is highly reminiscent of area preserving twist maps [24]. The nonsmooth invariant curves form barriers to the existence of dense orbits within the exceptional set. There has been some work on piecewise versions of the standard area preserving map; for example, see [9, 11, 31]. In certain cases these can be reduced to piecewise isometries [4]; we note that only discontinuous piecewise isometries can have nontrivial dynamics.

Such invariant curves were first noticed for a piecewise isometry in [3] at an isolated parameter value and in a rather small part of phase space. In this article we note a number of contrasts to the curves noted in [3]. First, the curves seem to appear over a large range of parameters and in particular are not limited to an isolated value of the rotation parameters.

Second, the curves can enclose a large proportion of the global attractor; in cases where they exist they seem to allow the possibility of highly complicated dynamics on the global attractor. Finally, we can observe that these curves appear on perturbations of circles on which there is nontrivial interval exchange dynamics.

A special case of the class of systems investigated here, for which the parameters are multiples of $\pi/5$, reduces to the “pentagon map” studied in [6] for a return map where the rotation angles are multiples of $\pi/5$. This latter system was found to have a natural renormalization scheme that divides phase space into a union of polygons filled with periodic points and a set foliated with a continuum of lines on which there are interval exchanges.

The rest of this paper is structured as follows. Section 2 defines the piecewise isometry T on $M = \mathbb{C}$ with atoms that are quadrants parametrized by two angles α_0, α_1 , two rotation centers h_0, h_1 , and two translations t_0 and t_1 . For the special case where $h_0 = h_1$ and $t_0 = t_1 = 0$, we characterize the dynamics of this map and show that its regular set is a union of two disks contained within a global attractor that consists of two larger disks. Its exceptional set is then a union of annuli. In section 3 we perturb the map so that $h_0 \neq h_1$, and we observe creation of chains of periodic islands within the exceptional set. These appear to be interleaved between nonsmooth invariant curves. Although we are not able to prove a continuation of any invariant sets within the exceptional set, some features do appear to persist. We also observe and discuss the appearance of invariant “fans” within the global attractor.

Section 4 shows (in Theorem 4.2) that the mapping has a global attractor that is geometrically simple (a union of two disks) in the special case of the parameters where $h_0 = h_1$ and the α_i/π are equal and irrational.

In section 5 we revisit a special case of the map introduced by Goetz in [14, 15, 16, 17, 18, 19] of the plane to itself with two half-plane atoms. For parameters such that the global attractor is a rhombus, we also find instances of nonsmooth invariant curves from numerical observations. The map arises as a local return map for a piecewise affine rotation on a torus also possessing a nonsmooth invariant curve. This also hints at the richness of the dynamics for the piecewise affine map studied, for example, in [1, 20] for an irrational value of the rotation parameter. We continue by discussing a number of conjectures and comments on the dynamics within the exceptional set. This includes a symbolic characterization of a subset contained within the global attractor that appears to contain most of the dynamics of interest.

2. A planar piecewise isometry with four quadrant atoms. We define a disjoint partition of \mathbb{C} into the usual four quadrants (Figure 2.1 (a))

$$\begin{aligned} P_0 &= \{z \mid \operatorname{Re}(z) > 0, \operatorname{Im}(z) \geq 0\}, \\ P_1 &= \{z \mid \operatorname{Re}(z) \leq 0, \operatorname{Im}(z) > 0\}, \\ P_2 &= \{z \mid \operatorname{Re}(z) < 0, \operatorname{Im}(z) \leq 0\}, \\ P_3 &= \{z \mid \operatorname{Re}(z) \geq 0, \operatorname{Im}(z) < 0\} \end{aligned}$$

(we will later disregard any points that land on the discontinuities, including $z = 0$) and four isometries

$$\begin{aligned} T_0(z) &= e^{i\alpha_0}(z - s_0) + s_0, \\ T_1(z) &= e^{i\alpha_1}(z - s_1) + s_1, \end{aligned}$$

$$\begin{aligned} T_2(z) &= e^{i\alpha_0}(z + 1 + t_0 - s_0) + s_0, \\ T_3(z) &= e^{i\alpha_1}(z - 1 + t_1 - s_1) + s_1, \end{aligned}$$

where the angles of rotations $\alpha_0, \alpha_1 \in [0, 2\pi)$, the centers $s_0, s_1 \in \mathbb{C}$, and the translations $1 + t_0, -1 + t_1 \in \mathbb{R}$ are parameters. We consider only t_i real to ensure that the map is invertible in a neighborhood of the s_i that crosses the real axis. We define the piecewise isometry $T : \mathbb{C} \rightarrow \mathbb{C}$ (illustrated schematically in Figure 1) by

$$(2.1) \quad T(z) = T_k(z) \iff z \in P_k.$$

We consider the case where

$$(2.2) \quad s_0 = \frac{1}{2} + ih_0, \quad s_1 = -\frac{1}{2} + ih_1,$$

and $h_0, h_1 \in \mathbb{R}$. This gives a family of piecewise isometries with six real parameters.¹ The system (2.1) clearly extends to more general cases, and some of these are conjugate under similarities, but we do not attempt a full classification of the maps; rather, we are concerned with highlighting several features of interest that we believe may be “typical” for families of piecewise isometries.

2.1. The “integrable” case $h_0 = h_1 = h$, $t_0 = t_1 = 0$. In this section we state and prove results for a special case when the centers of rotations are in the upper half-plane and they are symmetric with respect to the imaginary axis; see Figure 2(a). In this case, the dynamics is determined by three real parameters: the angular parameters α_0 and α_1 , and h . We will assume that h is nonnegative.

Define the circles $C_{r,0} = \{z : |z - ih - \frac{1}{2}| = r\}$, $C_{r,1} = \{z : |z - ih + \frac{1}{2}| = r\}$, and let

$$(2.3) \quad C_r = C_{r,0} \cup C_{r,1}.$$

Under these assumptions on the parameters, we will see that C_r is invariant for $r \leq \frac{1}{2}$; more precisely, we have the following.

Lemma 2.1. *For the parameters of the “integrable” case $h_0 = h_1 = h > 0$, $t_0 = t_1 = 0$, the following hold.*

- If $r < \min(\frac{1}{2}, h)$, then $T(C_{r,0}) = C_{r,0}$, $T(C_{r,1}) = C_{r,1}$, and each is simply a rotation by α_i about s_i .
- If $h < \frac{1}{2}$ and $h < r < \frac{1}{2}$, then $T(C_r) = C_r$, but the individual $C_{r,i}$ are not invariant.

This lemma enables one to characterize the dynamics of all points z inside $C_{\frac{1}{2}}$ and has as a consequence that all initial conditions in this region have ω -limit sets with dimension at most 1. The dynamics on the pair of circles C_r is conjugate to an IET. This exchange is equivalent to the interval exchange G_r on $[0, 4\pi)$ defined by

$$(2.4) \quad G_r(x) = \begin{cases} g(x + \alpha_0) & \text{if } x \in [0, 2\pi) \text{ and } h + r \sin(x) > 0, \\ g(x + \alpha_1) + 2\pi & \text{if } x \in [2\pi, 4\pi) \text{ and } h + r \sin(x) > 0, \\ g(x + \alpha_1) + 2\pi & \text{if } x \in [0, 2\pi) \text{ and } h + r \sin(x) < 0, \\ g(x + \alpha_0) & \text{if } x \in [2\pi, 4\pi) \text{ and } h + r \sin(x) < 0, \end{cases}$$

¹An interactive on-line simulation tool and movies illustrating the dynamics of this map are available at <http://dynamics.sfsu.edu/siam/>.

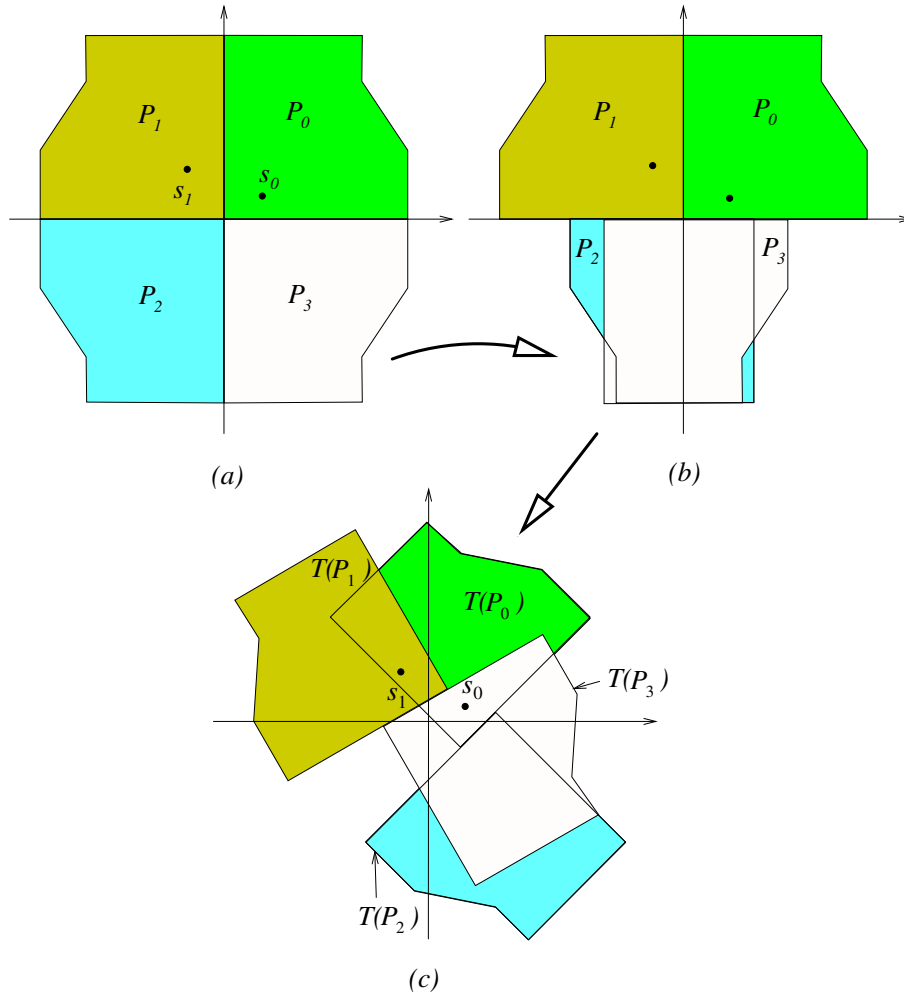


Figure 1. A schematic illustration of the action of T with atoms given by the four quadrants; we have $s_0 = \frac{1}{2} + ih_0$ and $s_1 = -\frac{1}{2} + ih_1$. The map T takes P_0 and rotates it by an angle α_0 about s_0 , and it rotates P_1 by α_1 about s_1 . The map first translates P_2 by the real number $1 + t_1$ and then rotates the image by α_1 about s_0 . Finally, T translates P_3 by $-1 + t_0$ and then rotates the image by α_1 . Note that t_i real means that $T(P_0) \cap T(P_2) = T(P_1) \cap T(P_3) = \emptyset$.

where $g(x) = x$ for $x \in [0, 2\pi)$ and g is 2π -periodic. As the reader may verify, the dynamics of G_r on $[0, 4\pi)$ and T on C_r is explicitly conjugate as follows.

Lemma 2.2. For $0 < r < \min(h, \frac{1}{2})$, the map T on C_r is conjugate to G_r via the map $c : [0, 4\pi) \rightarrow \mathbb{C}$:

$$c(x) = \begin{cases} \frac{1}{2} + ih + r \exp ix & : \text{ if } x \in [0, 2\pi), \\ -\frac{1}{2} + ih + r \exp ix & : \text{ if } x \in [2\pi, 4\pi). \end{cases}$$

We now consider the dynamics of the IET G_r . We say that α_i are *rationally independent* of 2π if there are no solutions of

$$k_0\alpha_0 + k_1\alpha_1 = 2\pi\ell$$

for $k_0, k_1 \in \mathbb{Z}^+$, and $\ell \in \mathbb{Z}$; in particular, α_i/π must both be irrational in this case. Note that an orbit of G_r taken modulo $[0, 2\pi)$ will consist of a composition of rotations.

Now define ξ_n to be the rotation undergone on the tangent space to a point starting at z_0 under the action of T (i.e., $\xi_n = \arg(DT^n(z_0))$ chosen as in (2.1)). We define upper and lower rotation numbers associated to the trajectory of z_0 under T by

$$\underline{R}(z) = \liminf_{n \rightarrow \infty} \frac{\xi_n}{n}, \quad \overline{R}(z) = \limsup_{n \rightarrow \infty} \frac{\xi_n}{n}.$$

If these are equal, we refer to both as the rotation number $R(z)$.

Lemma 2.3. *Suppose (without loss of generality) that $\alpha_0 < \alpha_1$; then for all $z \in \mathbb{C}$*

$$\alpha_0 \leq \underline{R}(z) \leq \overline{R}(z) \leq \alpha_1.$$

If $z \in C_r$ and IET G_r is uniquely ergodic, then

$$R(z) = \frac{\alpha_0 + \alpha_1}{2}$$

for almost all z .

Proof. This comes by noting that the action of T^n on a tangent vector is rotation k times by α_0 and $(n - k)$ times by α_1 , where $0 \leq k \leq n$. In the case of unique ergodicity, this must be with respect to a normalized Lebesgue measure on G_r that assigns equal measure to each of $C_{r,0}$ and $C_{r,1}$. Integration with respect to this measure gives the second result. ■

Remark 1. Consider the “integrable” case ($t_0 = t_1 = 0$ and $h_0 = h_1 = h$) such that $0 < h < \frac{1}{2}$.

- If $r < h$, then G_r is independent of r and consists of rotations on the two invariant intervals $[0, 2\pi)$ and $[2\pi, 4\pi)$.
- If $h = 0$, then G_r is independent of r .
- If $\alpha_i = p_i\pi/q_i$, then all orbits of G_r are periodic with period at most twice the least common multiple of q_1 and q_2 .
- If α_0 and α_1 are rationally independent of 2π , then there are no periodic orbits except when $r = 0$. To see this, observe that a periodic orbit x must satisfy $G_r^n(x) = x + 2\pi\ell$. Hence $x + k_0\alpha_0 + k_1\alpha_1 = x + 2\pi\ell$, which has no solution for α_i and 2π rationally independent.

For $h < r < \frac{1}{2}$, the dynamics of G_r is a nontrivial interval exchange on two circles with four intervals. We observe that these maps parametrized by α_0, α_1 , and r/h contain some surprising dynamics that in general is not fully understood.

If we let $\alpha_0 = \alpha_1 = \alpha$, our system can be naturally conjugated to \mathbb{Z}_2 skew products over irrational rotations studied first by Veech [29] and also by Keynes and Newton [22]. Define

$$\beta = \min(0, 2 \arccos(h/r))$$

and the map $f_{\alpha,\beta} : [0, 2\pi) \times \{0, 1\} \mapsto [0, 2\pi) \times \{0, 1\}$ by

$$(2.5) \quad (x, i) \mapsto (x + \alpha \pmod{2\pi}, i + \chi_{[0,\beta)}(x) \pmod{2}),$$

where $\chi_A(x)$ is the indicator function for the set A . The map $f_{\alpha,\beta}$ is conjugate to G_r via $\pi : [0, 2\pi) \times \{0, 1\} \rightarrow [0, 4\pi)$ given by

$$\pi(x, k) = x + 2\pi k - (\pi + \beta)/2 \pmod{4\pi}.$$

We now summarize a number of remarkable results that have been obtained for this family of maps. An irrational number $x \in (0, 1)$ is said to have *bounded quotients* if there is a K such that

$$x = \frac{1}{a_1 + \frac{1}{a_2 + \dots}}$$

for positive integers a_1, a_2, \dots , where $a_i < K$ for all i . The first results were obtained by Veech [29].

Theorem 2.4. *Assume that $\alpha/\pi \notin \mathbb{Q}$ and let B denote the uncountable Lebesgue zero measure set of all numbers $\theta \in (0, 2\pi)$ such that $\frac{\theta}{2\pi}$ has bounded partial quotients.*

1. Minimality [29]. *If $\beta/\alpha \notin \mathbb{Q}$, then the map $f_{\alpha,\beta}$ is minimal.*
2. Unique ergodicity for a residual set [29]. *For all $\alpha \in B$, $f_{\alpha,\beta}$ is uniquely ergodic.*
3. Nonunique ergodicity [29]. *For all $\alpha \notin B$, there exist uncountably many β 's such that $f_{\alpha,\beta}$ is not uniquely ergodic.*

Complementary results have been obtained for fixed β by Masur and Smillie [26] and more recently by Cheung and Boshernitzan [12].

Theorem 2.5 (see [25]). *Fix β . The set of all α such that $f_{\alpha,\beta}$ is not ergodic has Hausdorff dimension at most $1/2$.*

Theorem 2.6 (see [12]). *Fix $\beta \in B$ ($\frac{\beta}{2\pi}$ with bounded quotients). The set of α such that $f_{\alpha,\beta}$ is not ergodic has Hausdorff dimension precisely $1/2$.*

Theorem 2.7 (see [12]). *The set of all α for which $f_{\alpha,\beta}$ is not uniquely ergodic has zero Hausdorff dimension.*

3. Examples of dynamics and global attractors. If we perturb from the “integrable” case where the rotation centers have the same height and all dynamics is contained within one-dimensional invariant sets, we find a qualitative difference in dynamics even when $h_0 \approx h_1$. Figure 2 shows some trajectories for ten randomly selected points on the exceptional set within global attractor for $\alpha_0 = \alpha_1 = 1$ and $t_0 = t_1 = 0$. We show (a) and (b) $(h_0, h_1) = (0.25, 0.25)$, (c) $(0.25, 0.23)$, and (d) $(0.25, 0.2)$. Details of the invariant sets in (c) and (d) are shown in Figure 3(a) and (b), respectively. The trajectories show a high degree of complexity and some appear to enclose high period island chains. Others appear to be nonsmooth invariant circles—in particular, the trajectory of Figure 3(a) fourth from the bottom and the trajectory of Figure 3(b) third from the bottom. In all cases the nonsmooth invariant curves appear as barriers to movement of trajectories across them and in particular to ergodicity of the exceptional set.

To observe the appearance of dynamically fine structure as we perturb away from the “integrable” case, the movie [60539_01.mpg](#) illustrates an animated scan through parameter space given by fixing $\alpha_0 = \alpha_1 = -2\pi\gamma$, where $\gamma = \frac{\sqrt{5}-1}{2}$ is the golden mean, $t_0 = t_1 = 0$, and we linearly interpolate (h_0, h_1) along paths first from $(0, 0)$ to $(0.125, 0)$ and then from $(0.125, 0)$ to $(0.125, 0.25)$.² The white regions denote points that are not in the global attractor.

²Individual frames can be viewed on <http://dynamics.sfsu.edu/siam/>.

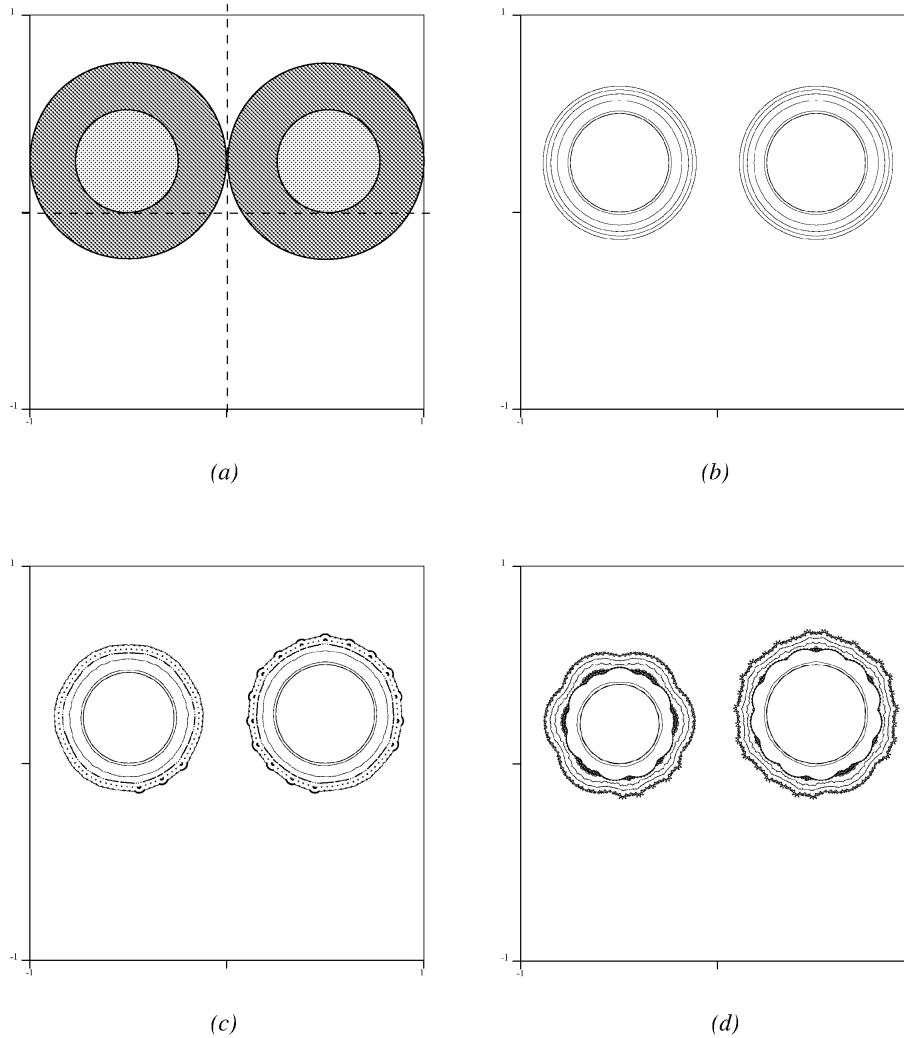


Figure 2. (a) The shaded region shows the global attractor for T with parameters $\alpha_0 = \alpha_1 = 1$, $(h_0, h_1) = (0.25, 0.25)$, and $t_0 = t_1 = 0$; the darker shaded area is the exceptional set $\bar{\mathcal{E}}$. (b) Ten trajectories in the exceptional set of the global attractor in (a) are shown; each trajectory moves according to an IET on the union of circles. (c) A near-integrable case with $(h_0, h_1) = (0.23, 0.25)$ and the same initial conditions. Some of the outer circles in (b) have broken into chains of periodic islands; one notes the presence of apparent nonsmooth invariant curves close to the previous circles. (d) A further perturbation with $(h_0, h_1) = (0.20, 0.25)$; for (b)–(d) 10^6 iterates were taken for ten initial conditions $(x, 10^{-10})$ for x chosen randomly in the range $[0.2, 0.8] + 0i$. In (a)–(d) the surrounding boxes show the region $[-1, 1] + i[-1, 1]$ of the complex plane.

The colors are assigned to points depending on their relative frequency of visiting one of the quadrants, namely, according to an approximated value of

$$\limsup_{N \rightarrow \infty} \frac{\#\{T^n x \in P_2 : 1 \leq n \leq N\}}{N}.$$

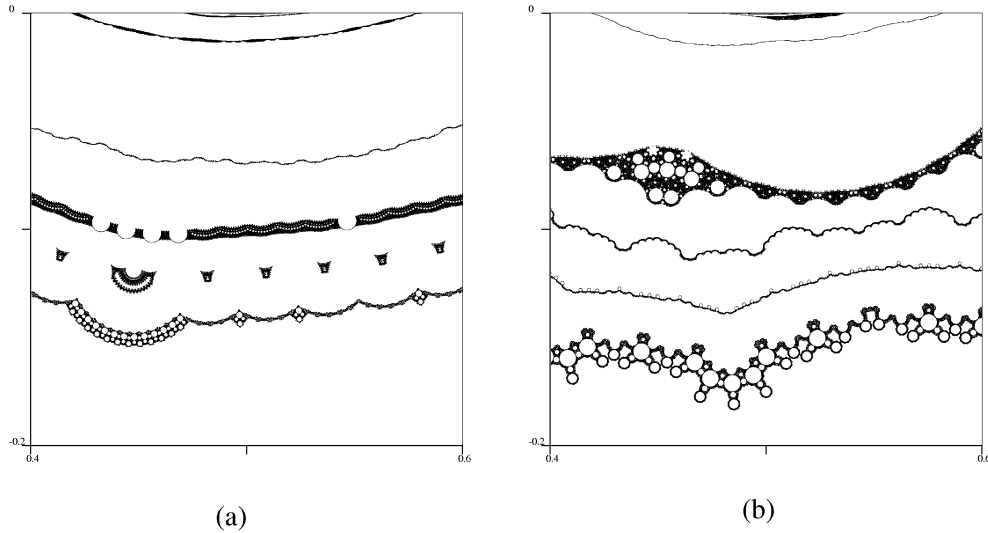


Figure 3. Figures (a) and (b) show details of Figure 2 (c) and (d) in the area $[0.4, 0.6] + i[-0.2, 0.0]$. Both images show the trajectories of ten initial conditions chosen as in Figure 2. Observe the presence of “nonsmooth invariant curves” and “stochastic layers” that are full of periodic islands approximately following the line of the invariant circles for the case $h_0 = h_1$.

Observe that an orbit of a periodic (or eventually periodic) cell is thus shaded using one color. This coloring scheme allows one to clearly identify and distinguish different periodic cells.

The “integrable” cases $(0, 0)$ occur at the start of the movie and $(0.125, 0.125)$ near the end of the movie. In both cases the global attractor consists of a simple pair of disks that are tangent at the imaginary axis. Observe the creation of very complicated global attractors on moving away from an “integrable” case. The periodic islands can be observed to be ejected by the global attractor to form extra connected components that are then gradually reduced in size by colliding with the discontinuity on the imaginary axis.

Figure 4 illustrates the structure of the global attractor for $h_0 = 0.05$, $h_1 = 0.0$, and $\alpha_0 = \alpha_1 = 2\pi\gamma$. The panels (a)–(d) show successive enlargements of regions of the images. We observe a very detailed structure of island chains. Figure 5 shows a dozen trajectories, iterated up to 10^6 times, within the global attractor.

The movie [60539.02.mpg](#) shows an animated zoom into the structure shown in Figure 4 (note that the sense of rotation is opposite to that in [60539.01.mpg](#)). Observe, in particular, the boundary of the global attractor that consists of several components—a main component with a very complicated boundary and a number of disks. Observe also that the main component does not appear to be simply connected; instead it encloses a number of holes.

3.1. Invariant fans within the global attractor. At one point in the movie sequence [60539.01.mpg](#) one can observe the brief appearance of a number of red “fans.” These are reproduced in Figure 6(a) for the particular case $\alpha = -2\pi\gamma$, $t_0 = t_1 = 0$, $h_0 = 0.07203725$, and $h_1 = 0$. The fans exchange according to the permutation

$$E \mapsto A \mapsto H \mapsto D \mapsto C \mapsto G \mapsto B,$$

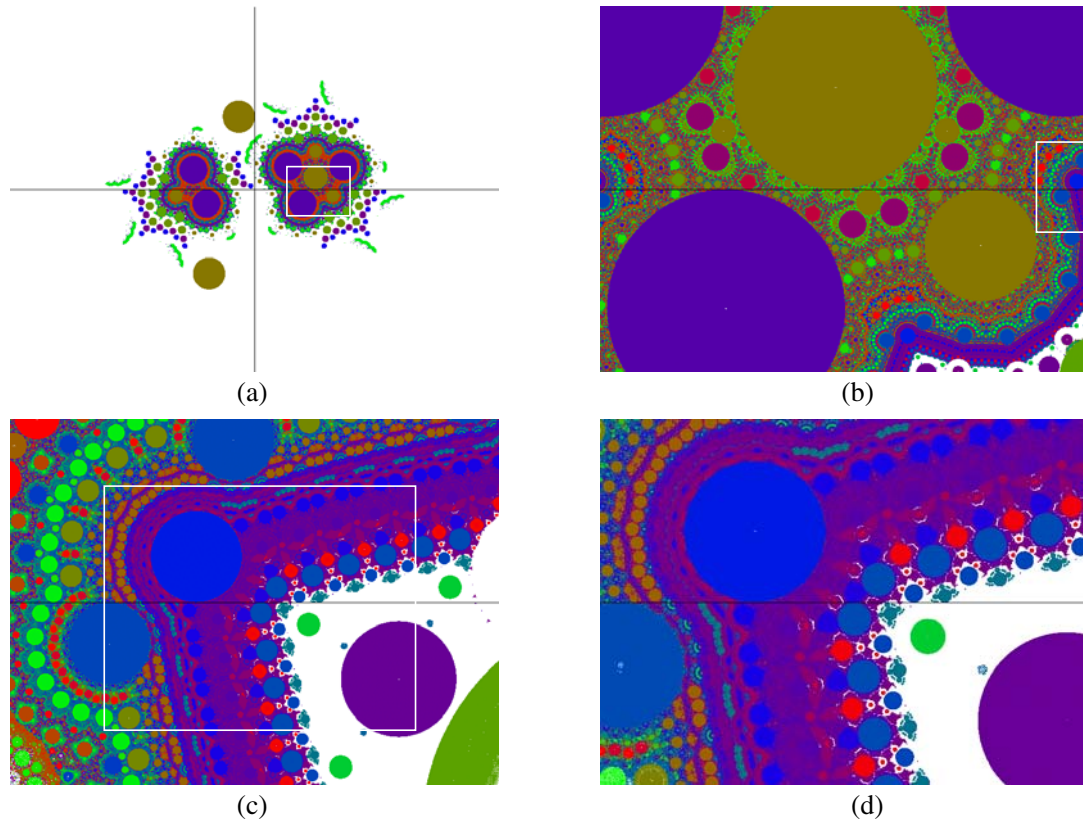


Figure 4. (a)–(d) show successive details of the dynamics on the global attractor for parameters $\alpha_0 = \alpha_1 = 2\pi\gamma$, $t_0 = t_1 = 0$, $h_0 = 0.05$, and $h_1 = 0$. The coloring corresponds to the average frequency of visits of an orbit to an upper-left quadrant. All orbits with the same eventually periodic itinerary are colored in one color. Observe the presence of a highly complex boundary on the global attractor, and observe that the attractor appears to contain a number of holes on a small scale. Clicking on the above images displays the associated movie (60539_02.mpg).

and then $B \cup F$ is mapped onto $E \cup F$.

Hence the first return map to $E \cup F$ consists of a simple exchange with rotation, giving orbits on a continuum of invariant arcs that foliate the fan $E \cup F$. The value of h_0 can be found by noting that the isometry $T_3(z)$ has a fixed point on the boundary of its domain of definition, namely, at $\tilde{z}_1 = -0.1944i$. The isometry

$$T_0 \circ T_2 \circ T_1 \circ T_1 \circ T_3 \circ T_0 \circ T_2$$

is also defined on some region as can be verified from the Figure 6(b,c), and this has a fixed point at $\tilde{z}_2 = -(1.322389h_0 + 0.09914)i$. From this it can be determined that the two fixed points coincide (at $\tilde{z} = \tilde{z}_1 = \tilde{z}_2$) when $h_0 = 0.07203725$.

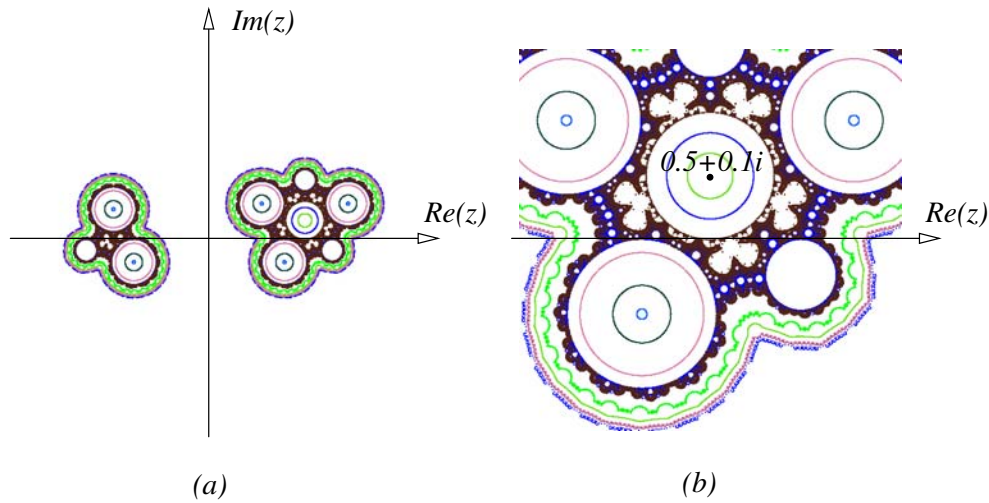


Figure 5. Trajectories of T at same parameters as in Figure 4. We show trajectories of a small selection of initial conditions; each color signifies a different trajectory. (a) shows the square $[-1, 1] + i[-1, 1]$, while (b) shows $[0.3, 0.7] + i[-0.2, 0.2]$. Observe the presence of “nonsmooth invariant curves” and “stochastic layers” that are not so obvious in Figure 4.

Proposition 3.1 (invariant fans). Let $h_0 = 0.07203725$, $h_1 = 1$, $t_0 = t_1 = 0$, and $\alpha_0 = \alpha_1 = -2\pi\gamma$. Let

$$F = \{z \in \mathbb{C} \mid \pi/2 \geq \arg(z - \tilde{z}) > -0.4790168, \quad |z - \tilde{z}| < 0.1944\},$$

$$E = \{z \in \mathbb{C} \mid 3.9707596 \geq \arg(z - \tilde{z}) > \pi/2, \quad |z - \tilde{z}| < 0.1944\}$$

be as illustrated in Figure 6(b). Then the return map of T to the union of $E \cup F$ acts as an exchange on the two fans E and F :

$$T_{E \cup F} = \begin{cases} T_0 \circ T_2 \circ T_1 \circ T_1 \circ T_3 \circ T_0 \circ T_2 & \text{if } z \in E, \\ T_3 & \text{if } z \in F. \end{cases}$$

As a consequence, there is a dense set of preimages of the discontinuities within the set of fans. To our knowledge this is the first example in the literature of a piecewise isometry that has open sets within the exceptional set with a mixture of curved and straight boundaries. Previous examples in [5, 6] are bounded by polygons.

3.2. Persistence of nonsmooth invariant curves. Previous work on the dynamics of piecewise isometries has noted that they can bear close resemblances to Hamiltonian (area preserving) dynamics [27, 28]; see [24]. Our numerical experiments suggest that the analogy may be even closer than previously suspected. Perturbations from an “integrable” case $\epsilon = 0$ are typically associated with the appearance of rings of very small periodically coded islands. This behavior is analogous to that given by the Poincaré–Birkhoff theorem for smooth area preserving maps. However, we note that there are no periodic points for any G_r (except possibly on the map discontinuities), and Poincaré–Birkhoff cannot be applied in this context. Moreover, for many small perturbations of ϵ it appears that some of the invariant curves on

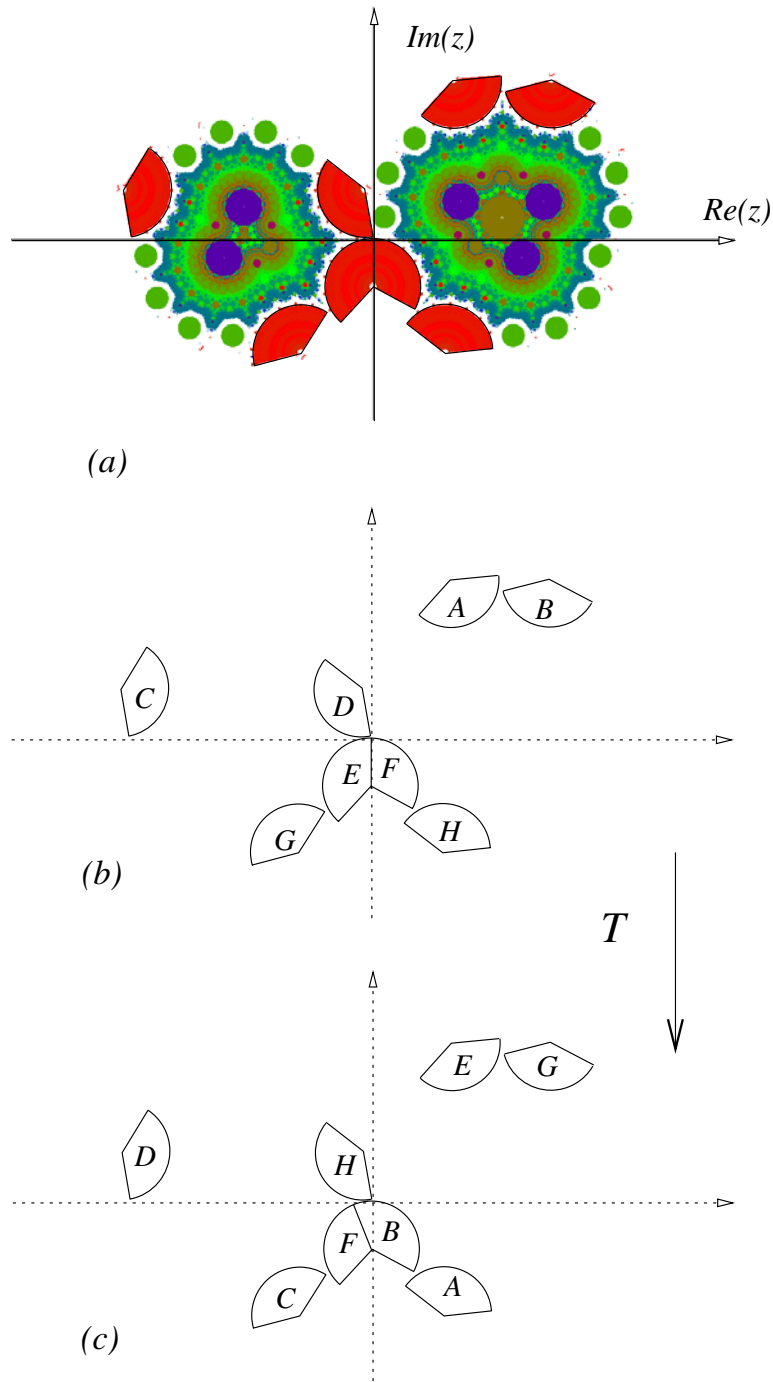


Figure 6. An example that occurs in 60539.01.mpg has an exceptional set that contains open “fans” for $\alpha_0 = \alpha_1 = -2\pi\gamma$, $t_0 = t_1 = h_1 = 0$, and $h_0 = 0.07203725$. There is an exchange on the fans in (a) labeled A–H in (b). These are mapped onto themselves by the map T as shown in (c) which leads to a first return on $E \cap B$ that is conjugate to a rotation on a continuum of concentric arcs.

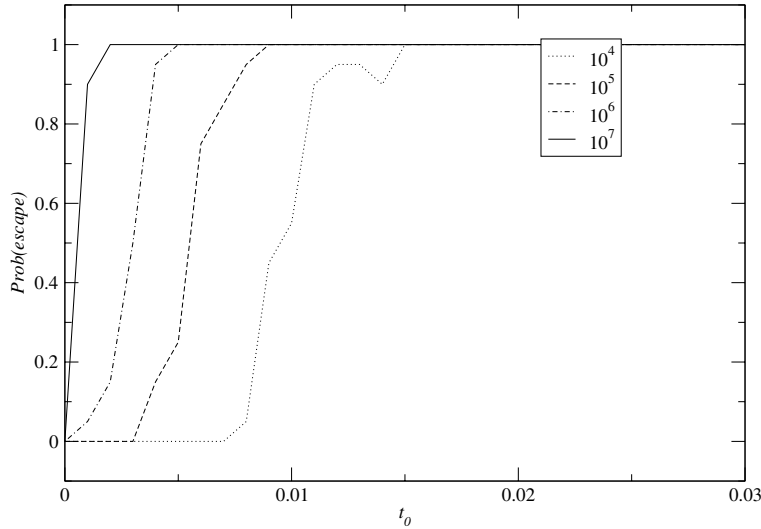


Figure 7. Plots showing probability P of escape from a neighborhood of the period-one cell centered at $s_0 = \frac{1}{2} + ih_0$. We set $\alpha_i = 1$, $(h_0, h_1) = (0.005, 0)$, $t_1 = 0$ and vary t_0 . Twenty random initial conditions are chosen just outside the period-one cell, and the proportions that escape to a distance at least 0.1 from the cell are plotted. Observe that, for increasing length of trajectory, if $t_0 \neq 0$, then all trajectories escape, while for $t_0 = 0$ none escape.

which IETs occur may actually persist to become “nonsmooth” invariant curves. This is analogous to the persistence of invariant curves for smooth area preserving maps as predicted by the Kolmogorov–Arnol’d–Moser theorem.

We have tried to detect the appearance of nonsmooth invariant curves near the period-one cell by studying a set of twenty trajectories started at random points on the discontinuity just outside a period-one cell. If the trajectory on its return to P_0 moves to an order-one distance from the period-one cell, then we say *it escapes*. Figure 7 shows that, fixing $t_1 = 0$, the curves appear to exist only in the case $t_0 = 0$. Other numerical experiments suggest that the invariant curves can exist for a set of parameter values for (2.1), where $t_0 = t_1$, i.e., for a set of parameter values of codimension at most one.

We are at a loss as to how to explain these invariant curves, but because of Theorem 2.4 and the discussion immediately thereafter, we believe they may be connected to the break-up of minimal nonergodic interval exchanges that appear in the “integrable” case. The fact that they appear for some parameter values but not for others may be associated with a symmetry of the map that we have not been able to identify as yet.

4. Global attractors for the “integrable case” of the quadrant map. In this section we show that for all choices of s_0, s_1 and angles $\alpha = \alpha_0 = \alpha_1$ incommensurate with π , the piecewise rotation T has a global attractor (Theorem 4.2). Moreover, if the heights of the centers of rotations are the same ($s_0 = \frac{1}{2} + ih$, $s_1 = -\frac{1}{2} + ih$), then up to a set of measure zero the attractor is the union of two disjoint disks.

Definition 4.1 (global attractor). *The global attractor for the map $T : X \mapsto X$ is*

$$\tilde{M} = \bigcup_{x \in X} \omega(x),$$

where $\omega(x)$ denotes the set of accumulation points of the T -orbit of x . The set \tilde{M} is the bounded global attractor for T if \tilde{M} is bounded.

Note that our definition of global attraction is slightly unusual; this is simply for convenience in the results below. In particular, the maximal Milnor attractor (the smallest compact set containing the ω -limit set of all full measure sets) is contained within the closure of this set.

Remark 2. Observe that since T is continuous on the interior of each quadrant and since we ignore a countable union of lines whose forward orbits are the boundaries of the quadrants, the set \tilde{M} is invariant under T except for a set of zero measure.

In the subsequent results we use the fact that map T has a bounded global attractor if and only if that there is a constant $K > 0$ such that

$$\limsup_{n \rightarrow \infty} |T^n x| < K \text{ for all } x.$$

Theorem 4.2 (existence of a bounded attractor). *For all choices of s_0, s_1 , $\alpha = \alpha_0 = \alpha_1$ incommensurate with π and $t_0 = t_1 = 0$, the piecewise rotation T has a bounded global attractor.*

In order to prove Theorem 4.2 we use a general result presented in [8]. Since $\alpha = \alpha_0 = \alpha_1$ is incommensurate with π , at infinity, the piecewise rotation essentially behaves as a uniquely ergodic irrational rotation on the circle. This is used in the computation of the average drift or attraction of an orbit to the origin. Computations in [8] yield that the piecewise rotation is globally attracting if

$$(4.1) \quad \int_0^{2\pi} \lim_{R \rightarrow \infty, x = Re^{\theta i}} (|Tx| - |x|) \, d\theta < 0.$$

The same technical estimates apply here in the case of the map T with four atoms. Hence in order to prove Theorem 4.2 it suffices to show that the above integral is negative. Actually, as the following computation illustrates, it turns out that the integral (4.1) is constant; and it does not depend on the angle of rotation α , nor does it depend on the position of s_0 and s_1 . The computation is divided into two lemmas.

Lemma 4.3. *For $i = 1, \dots, 4$ and any θ , if $x = Re^{\theta i}$, then*

$$(4.2) \quad \lim_{R \rightarrow \infty} (|T_i x| - |x| - f_i(\theta)) = 0,$$

where

$$f_i(\theta) = \frac{1}{2} \left(c_i \sigma^{-1} (\rho^{-1} - 1) + \bar{c}_i \sigma (\rho - 1) \right),$$

and $\sigma = e^{\theta i}$, $\rho = e^{\alpha i}$, and numbers c_i denote the centers of rotations for T_i .

We remark that the c_i are given by

$$(4.3) \quad c_0 = s_0, \quad c_1 = s_1, \quad c_2 = s_0 + \frac{\rho}{1 - \rho}, \quad c_3 = s_1 - \frac{\rho}{1 - \rho}.$$

Proof of Lemma 4.3. Note that

$$(4.4) \quad |Tx| = |\rho(R\sigma - c_i) + c_i| = |\rho\sigma| \left| R + c_i\sigma^{-1}(\rho^{-1} - 1) \right| = \left| R + c_i\sigma^{-1}(\rho^{-1} - 1) \right|.$$

The lemma follows from the fact that for any $z \in \mathbb{C}$

$$(4.5) \quad \lim_{R \rightarrow \infty} (|R + z| - R - \operatorname{Re}(z)) = 0$$

by substituting $z = c_i\sigma^{-1}(\rho^{-1} - 1)$ in (4.5). ■

Lemma 4.4. *Let $f(\theta)$ be defined as follows:*

$$(4.6) \quad f(\theta) = \begin{cases} f_0(\theta) & \text{if } 0 \leq \theta < \frac{\pi}{2}, \\ f_1(\theta) & \text{if } \frac{\pi}{2} \leq \theta < \pi, \\ f_2(\theta) & \text{if } \pi \leq \theta < \frac{3\pi}{2}, \\ f_3(\theta) & \text{if } \frac{3\pi}{2} \leq \theta < 2\pi. \end{cases}$$

Then

$$\int_0^{2\pi} f(\theta) d\theta = -2.$$

Proof. First we compute the antiderivative

$$F_i(\theta) = \int f_i(\theta) d\theta = \frac{i}{2} (\rho - 1) \left(\sigma \bar{c}_i + \sigma^{-1} \rho^{-1} c_i \right).$$

The definite integral can then be computed as follows:

$$\begin{aligned} \int_0^{2\pi} f(\theta) d\theta &= (F_0(\frac{\pi}{2}) - F_0(0)) + (F_1(\pi) - F_1(\frac{\pi}{2})) \\ &\quad + (F_2(\frac{3\pi}{2}) - F_2(\pi)) + (F_3(2\pi) - F_3(\frac{3\pi}{2})) \\ &= \frac{i+1}{2} (\rho - 1) \left(s_0 - is_1 - c_2 + ic_3 - i\rho^{-1}(s_0 - is_1 - c_2 + ic_3) \right) \\ &= \frac{i+1}{2} (\rho - 1) \left(\overline{\left(\frac{(i+1)\rho}{\rho-1} \right)} - i\rho^{-1} \frac{(i+1)\rho}{\rho-1} \right) \\ &= -2. \end{aligned}$$

In the penultimate line of the above computation we have used (4.3). Since $\int_0^{2\pi} f(\theta) d\theta = -2 < 0$, the piecewise rotation T is globally attracting. This concludes the proof of Theorem 4.2. ■

Remark 3. One may define a “rate of repulsion from infinity” as follows:

$$\operatorname{rate}(x) = \lim_{N \rightarrow \infty} \lim_{|x| \rightarrow \infty} \frac{|T^N x| - |x|}{N}.$$

We have computed that $\operatorname{rate}(x) = \frac{1}{2\pi} \int f(\theta) d\theta = -1/\pi$ is constant for large enough x .

Theorem 4.2 states that the set of accumulation points for the piecewise rotation T is bounded. As illustrated in previous sections of this paper, in general the accumulation set is mysterious and complicated. However, in the particular “integrable” case with $s_0 = 1/2 + hi$,

$s_1 = -1/2 + hi$, where $h \in \mathbb{R}$, we are able to determine precisely that all points are attracted to the invariant set $\Omega = D(s_0, 1/2) \cup D(s_1, 1/2) \cup Z$, which is the union of two unit disks centered at s_0 and s_1 , respectively, and a set Z of zero measure.

Theorem 4.5 (global attractor, integrable case). *Let $s_0 = 1/2 + hi$, $s_1 = -1/2 + hi$, $t_0 = t_1 = 0$, and $\alpha_0 = \alpha_1 = \alpha$ with α incommensurate with π . Then the global attractor for T is*

$$\Omega = D(s_0, 1/2) \cup D(s_1, 1/2) \cup Z,$$

where Z has zero (two-dimensional) Lebesgue measure.

Proof. The proof consists of three parts. First, observe that every point x in $D(s_0, 1/2) \cup D(s_1, 1/2)$ is an accumulation point for the orbit of x . This is because the map restricted to the two circles $\partial D(s_0, |x - s_0|)$ and $\partial D(s_1, |x - s_1|)$ is conjugate to an interval exchange and all except finitely many points are recurrent for any interval exchange [21].

Next, define the ‘‘Lyapunov’’ function $L(x) = \min\{|s_0 - x|, |s_1 - x|\}$ for $x \in \mathbb{C}$. We wish to show that for all $x \notin \Omega$,

$$(4.7) \quad L(Tx) \leq L(x).$$

Since on P_0 , T acts as a rotation about s_0 , it follows that for all $x \in P_0$

$$(4.8) \quad \begin{aligned} L(Tx) &= \min\{|s_0 - Tx|, |s_1 - Tx|\} \\ &= \min\{|s_0 - x|, |s_1 - Tx|\} \leq |s_0 - x| = L(x). \end{aligned}$$

Similarly, if $x \in P_1$, $L(Tx) \leq L(x)$ since s_0 and s_1 are symmetric with respect to the imaginary line. Suppose that $x \in P_2$. Since T acts on P_2 as a translation by the unit, $1 = s_0 - s_1$, followed by the rotation about s_1 ,

$$(4.9) \quad \begin{aligned} L(Tx) &= \min\{|s_0 - Tx|, |s_1 - Tx|\} \\ &= \min\{|s_0 - \rho(x - s_1) - s_0|, |s_1 - Tx|\} \\ &= \min\{|s_1 - x|, |s_1 - Tx|\} \leq |s_1 - x| = L(x). \end{aligned}$$

Similarly, if $x \in P_3$, then one can verify that $L(Tx) \leq L(x)$. This means that $\{L(T^n x)\}_{n \geq 0}$ is nondecreasing, bounded below, and hence has a limit as $n \rightarrow \infty$. Consider any x and let $R = \lim_{n \rightarrow \infty} L(T^n x)$; then necessarily $\omega(x) \subset L^{-1}(R)$.

The second part of the proof aims to show that the set of recurrent points on $L^{-1}(R)$ has zero Lebesgue measure for almost all $R > \frac{1}{2}$. Suppose that $R > \frac{1}{2}$ and define

$$E(R) := ((P_0 \cup P_3) \cap \partial D(s_0, r_x)) \cup ((P_1 \cup P_2) \cap \partial D(s_1, r_x)) = L^{-1}(R).$$

Geometrically, the set E is a union of arcs, meeting at two points on the imaginary axis for $R > \frac{1}{2}$ and resembling a ‘‘pair of spectacles’’ when $R = \frac{1}{2}$. Note that $L^{-1}(R) = C_R$ (2.3) for $R \leq \frac{1}{2}$. Let $\tilde{E}(R)$ be the set of points within E that are recurrent and denote one-dimensional Lebesgue measure by ℓ_1 .

For all points $z \in E$ such that $T(z)$ remains within E , the map T is conjugate to G_R and hence to $f_{\alpha, \beta}$ with $\beta = \min(0, 2 \arccos(h/R))$ depending explicitly on R . As a special case of Theorem 2.4(1) we have that $f_{\alpha, \beta}$ is minimal for almost all β , namely, for those such that

$\beta \notin \alpha\mathbb{Q}$. The set of $\beta \neq 0$ that gives nonminimal $f_{\alpha,\beta}$ has zero measure, and hence the set of $R > \max(\frac{1}{2}, h)$ that gives G_R nonminimal has zero measure. Since G_R being minimal means that almost all points starting on E must leave it after a finite number of iterates, we can conclude that

$$\ell_1(\tilde{E}(R)) = 0$$

for all R in this full measure set.

If $h < \frac{1}{2}$, we are done. In the case that $h > \frac{1}{2}$, we note that for $h \geq R > \frac{1}{2}$ we have $\beta = 0$. In this case the map G_R is transitive and dense on each of the circles $\partial D(s_i, R)$, and hence also in this case $\tilde{E}(R)$ is empty. In either case, the set of recurrent points is contained within the set

$$\bigcup_{R > \frac{1}{2}} \tilde{E}(R),$$

and by Fubini’s theorem this has zero two-dimensional measure. Hence, the set of recurrent points on $L^{-1}(R)$ has zero Lebesgue measure for almost all $R > \frac{1}{2}$.

Finally, $T(\Omega) = \Omega$ up to a set of zero measure by Remark 2, and since T as a piecewise isometry may only decrease measure, T must be almost everywhere 1-1. Thus T preserves a finite Lebesgue-equivalent two-dimensional measure on any subset of the global attractor Ω . By Poincaré recurrence, Ω must contain a full measure subset of recurrent points; this completes the proof. ■

5. Discussion. We discuss a number of disparate topics related to the dynamics of the piecewise isometries such as (2.1). First, we note that nonsmooth invariant curves can appear in piecewise isometries with only two atoms. Next, we show that under fairly general assumptions one cannot find invariant curves that are just a union of curved arcs formed from boundaries of periodic cells. We then discuss the aspects of the coding of the orbits that appears to contain most of the “interesting” dynamics, and we conclude with a summary of a few of the open questions this work raises, particularly as related to the existence and stability of nonsmooth invariant curves.

5.1. Nonsmooth invariant curves for a piecewise isometry with two atoms. The map introduced by Goetz [14] also shows evidence of nonsmooth invariant curves for certain parameter values. In particular, we consider $S : \mathbb{C} \rightarrow \mathbb{C}$ defined by

$$(5.1) \quad S(z) = \begin{cases} e^{i\theta}(z - s_0) + s_0 & \text{for } \operatorname{Re}(z) \geq 0, \\ e^{i\theta}(z - s_1) + s_1 & \text{for } \operatorname{Re}(z) < 0, \end{cases}$$

where we fix

$$s_0 = 0.3872983 + 0.5i, \quad s_1 = -0.1936491 + 0.25i, \quad \theta = -1.8234765.$$

(We note that $\theta = \arccos(-0.25)$.) Figure 8 illustrates that the global attractor is a rhombus $ABCD$ that intersects both axes and in particular the discontinuity OB . The parameter values can be calculated by observing that this map is a piecewise isometry in PWI(3,3) of class II_d as defined in [5], and so this map is specified (up to similarity) by the rotation θ . We

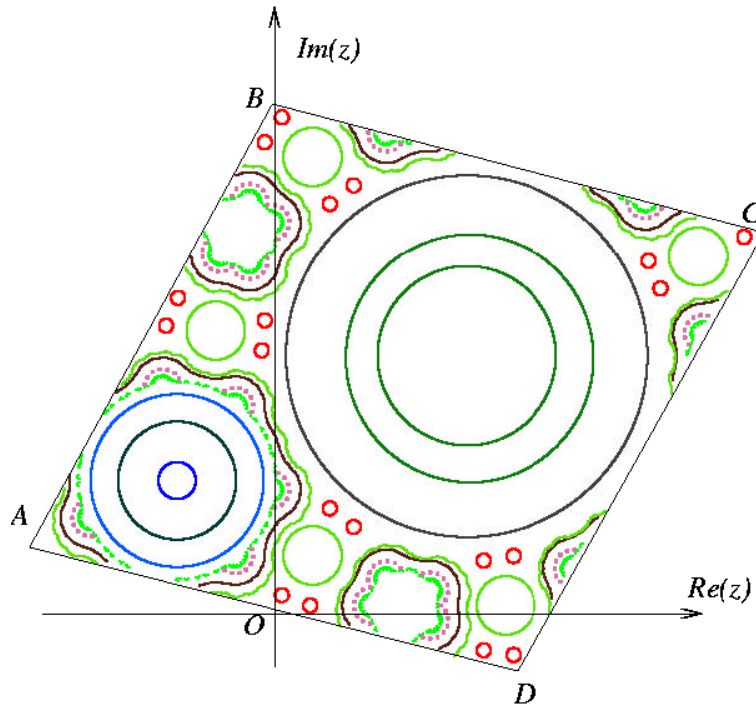


Figure 8. The global attractor $ABCD$ for the map S (5.1); see text for parameter values. Note that the global attractor consists of a rhombus; several trajectories are illustrated in different colors. There appear to be many families of nonsmooth invariant curves in the exceptional set of this map.

show the trajectories of a number of initial conditions on the global attractor, each of which is shown in a different color.

In fact, the phenomena of nonsmooth invariant circles for PWIs was observed first in [3] for a map of $[-1, 1]^2$ to itself defined by

$$(x, y) \mapsto (y, g(-x + ay))$$

with $g(x) = x$ for $x \in [-1, 1]$, $g(x + 2) = g(x)$, and parameter $a = 2 \cos \theta$. This map can be viewed, after a linear shear of the coordinates, as a one-parameter family of PWIs parametrized by $\theta \in \mathbb{R}$. In the case $\theta = \arccos(0.25)$ one can find small regions of $[-1, 1]^2$ apparently enclosed by a series of nonsmooth invariant circles.

5.2. Jordan curves composed of unions of circular segments are not invariant. In the absence of any positive argument of the existence of the nonsmooth invariant curves, we demonstrate that under general conditions, they cannot be composed of a union of segments of boundaries of circular cells. In particular, we have the following.

Lemma 5.1. Consider $x \in \bar{\mathcal{E}}$ and a periodic cell D with period p such that the return to D is an irrational rotation. If $\omega(x) \cap \partial D$ contains an interval, then

$$\omega(x) \cap \partial D = \partial D.$$

Proof. Suppose $\omega(x) \cap \partial D = W$ with W contains some interval in ∂D . Thus, there is an $N > 0$ such that

$$\bigcup_{n=1}^N T^{pN}(W) \supseteq \partial D \setminus Q,$$

where Q is a finite set consisting of points in ∂D that land on the discontinuity after at most pN iterates. Pick any $q \in \partial D \setminus Q$ and note that there is a $\tilde{q} \in W$ such that $T^k(\tilde{q}) = q$ with $k \leq pN$ and \tilde{q} is a point of continuity of T^k for all $1 \leq k \leq pN$. We then note that for a sequence $T^{l_j}(x) \rightarrow \tilde{q}$ we have $T^{l_j+k}(x) \rightarrow q$, and this gives the conclusion of Lemma 5.1. ■

Lemma 5.1 gives rise to the following theorem, which excludes the possibility that the invariant curves consist (for example) of the boundary of a connected component of the plane bounded by a ring of tangent periodic disks.

Theorem 5.2. *Suppose that $C = \omega(x)$ is a continuous embedding of a circle into the exceptional set $\bar{\mathcal{E}}$ that is not the boundary of a periodic cell. Then C cannot contain any curved segments from periodic cells.*

Proof. Lemma 5.1 shows that such a circle contains either the whole of the boundary of a periodic cell, or no interval within the boundary of that cell. ■

We observe that Theorem 5.2 does not preclude the possibility that unions of segments from ellipses form invariant curves for more general piecewise affine maps; these have been observed in recent work [23] on a piecewise affine map with two pieces.

5.3. Symbolic dynamics for T on the global attractor. We wish to demonstrate in this section that the invariant curves observed in the map T defined by (2.1) do not require or use the lack of invertibility of T . The map $T : \mathbb{C} \rightarrow \mathbb{C}$ defined by (2.1) induces a symbolic dynamics through the correspondence between $z \in \mathbb{C}$ and the symbol sequence

$$\iota(z) = \{s_k\} \in \Sigma^+ = \{0, 1, 2, 3\}^{\mathbb{N}}$$

such that $\bar{s}_k = l$ if and only if $T^k(z) \in P^l$. Note that only a zero entropy subshift is coded by orbits of T [10]. The shift operator $\sigma : \Sigma^+ \rightarrow \Sigma^+$ is semiconjugate to T , $\iota(T(z)) = \sigma(\iota(z))$, and the set

$$\Sigma_1^+ = \iota(\mathbb{C})$$

characterizes all *admissible* sequences for the map T . Now consider the set

$$\Sigma_2^+ = \Sigma_1^+ \cap \Sigma_A^+,$$

where A is the matrix

$$A = \begin{pmatrix} 1 & 0 & 1 & 1 \\ 0 & 1 & 0 & 0 \\ 0 & 1 & 0 & 0 \\ 1 & 0 & 1 & 1 \end{pmatrix}$$

and the subshift is defined by $\Sigma_A^+ = \{\mathbf{s} : A_{s_k, s_{k-1}} = 1 \text{ for all } k \in \mathbb{N}\}$. We extend these definitions to two-sided time and write the corresponding sets by dropping the “+.” The following lemma shows that orbits in Σ_2^+ have unique backward orbits in Σ_2 .

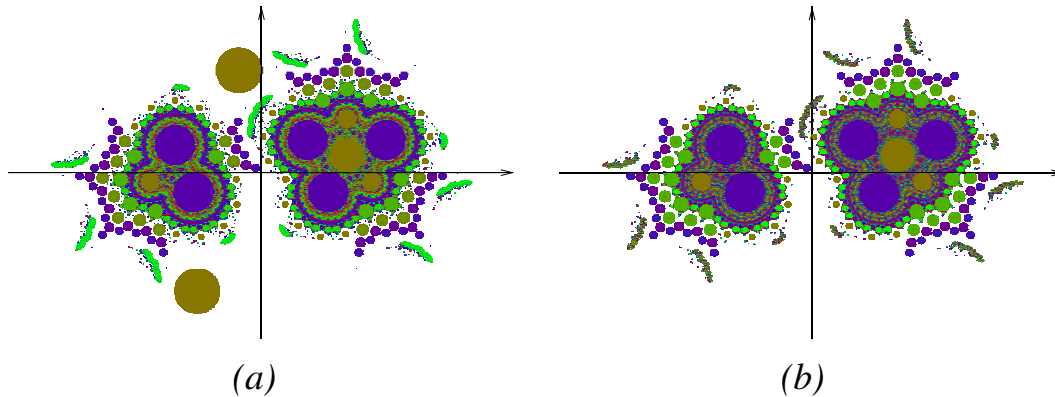


Figure 9. (a) The global attractor for $\alpha = -2\pi\gamma$, $t_0 = t_1 = h_1 = 0$, and $h_0 = 0.05$ (see Figure 4(a)); (b) shows the subset of the global attractor that disregards points with codings not lying in Σ_A^+ . We conjecture this contains everything in (a) except for a finite set of periodically coded islands.

Lemma 5.3. *Suppose that $s^+ = \iota(z) \in \Sigma_2^+$. Then there is at most one $s \in \Sigma_2$ such that $s_i^+ = s_i$ for $i \geq 0$.*

Proof. First, suppose that $z \in \mathbb{C}$ is such that $z \in T(\mathbb{C})$; then we claim that

$$\#\{w : \iota(w) \in \Sigma_A^+ \ \& \ T(w) = z\} = 1.$$

Note that $T(P_1) \cap T(P_2) = \emptyset$ and $T(P_0) \cap T(P_3) = \emptyset$. Assume that $z \in P_0$ and $T(w) = z$. If $\iota(w) \in \Sigma_A^+$, then $w \in P_0$ or $w \in P_3$, but $T(P_0) \cap T(P_3) = \emptyset$, and so only one such w can exist. Similar arguments apply in the case that z lies in one of the other atoms. Hence there is at most one w such that $T(w) = z$ and $\iota(w) \in \Sigma_2^+$. By induction we can choose at most one backward trajectory through w with coding lying in Σ_2 . ■

As a direct consequence we can characterize the symbolic dynamics of a subset of the global attractor.

Theorem 5.4. *The set $\iota^{-1}(\Sigma_2)$ is contained within the global attractor.*

In fact, for the parameter range considered this set seems to contain a large proportion of the measure of the global attractor. Figure 9 illustrates this for the numerically obtained attractor for parameters given in the figure caption. (a) shows the global attractor for the map (2.1), while (b) shows only the subset of the attractor obtained when we disregard all trajectories that do not give a coding lying in Σ_A^+ .

5.4. Open problems. The examples presented here are highly suggestive that the non-smooth invariant curves are real dynamical effects. However, in the absence of a single example in which we can prove that they exist, one clearly needs to proceed with great caution. We highlight a few of the many intriguing open problems:

- Can one find a nontrivial but rigorously provable example of a nonsmooth invariant curve for any PWI?
- Can one quantify the codimension of parameter values for which one typically finds these curves?
- More precisely, can one use a perturbed map in the neighborhood of the map G_r in (2.4) to find conjugacies between periodic orbits and invariant graphs?

- What is the role of Diophantine properties of the rotation number in determining the dynamics on the exceptional set near the “integrable” case? The analogy with smooth area preserving maps and Theorem 2.4 would suggest that these are very important.

Acknowledgments. We thank the London Mathematical Society for a visitors grant that allowed Arek Goetz to visit Peter Ashwin at Exeter in March 2002 during which this work commenced. Both authors thank the University of Marseille-Luminy for hosting visits of Arek Goetz and Peter Ashwin. We thank Xin-Chu Fu, Michael Boshernitzan, Yitwah Cheung, and Franco Vivaldi for their perceptive and helpful comments on this work. We would also like to thank Jim Swift for sharing some unpublished examples of nonsmooth invariant circles.

REFERENCES

- [1] R. L. ADLER, B. KITCHENS, AND C. TRESSER, *Dynamics of non-ergodic piecewise affine maps of the torus*, Ergodic. Theory Dynam. Systems, 21 (2001), pp. 959–999.
- [2] R. L. ADLER, B. KITCHENS, M. MARTENS, C. TRESSER, AND C. W. WU, *The mathematics of halftoning*, IBM J. Res. Develop., 47 (2003), pp. 5–15.
- [3] P. ASHWIN, *Nonsmooth invariant circles in digital overflow oscillations*, in Proceedings of the 4th International Workshop on Nonlinear Dynamics of Electronic Systems, Seville, Spain, 1996, pp. 417–422.
- [4] P. ASHWIN, *Elliptic behaviour in the sawtooth standard map*, Phys. Lett. A, 232 (1997), pp. 409–416.
- [5] P. ASHWIN AND X.-C. FU, *On the geometry of orientation-preserving planar piecewise isometries*, J. Nonlinear Sci., 12 (2001), pp. 207–240.
- [6] P. ASHWIN AND A. GOETZ, *Polygonal invariant curves for a planar piecewise isometry*, Trans. Amer. Math. Soc., 2005, to appear.
- [7] M. BOSHERNITZAN AND I. KORNFELD, *Interval translation mappings*, Ergodic. Theory Dynam. Systems, 15 (1995), pp. 821–832.
- [8] M. BOSHERNITZAN AND A. GOETZ, *A dichotomy for a two-parameter piecewise rotation*, Ergodic. Theory Dynam. Systems, 23 (2003), pp. 759–770.
- [9] S. BULLETT, *Invariant circles for the piecewise linear standard map*, Comm. Math. Phys., 107 (1986), pp. 241–262.
- [10] J. BUZZI, *Piecewise isometries have zero topological entropy*, Ergodic. Theory Dynam. Systems, 21 (2001), pp. 1371–1377.
- [11] N. I. CHERNOV, *Ergodic and statistical properties of piecewise linear hyperbolic automorphisms of the 2-torus*, J. Statist. Phys., 69 (1992), pp. 111–134.
- [12] Y. CHEUNG, *Hausdorff dimension of the set of nonergodic directions (with an appendix by M. Boshernitzan)*, Ann. of Math. (2), 158 (2003), pp. 661–678.
- [13] A. C. DAVIES, *Nonlinear oscillations and chaos from digital filters overflow*, Phil. Trans. Roy. Soc. A, 353 (1995), pp. 85–99.
- [14] A. GOETZ, *Dynamics of Piecewise Isometries*, Ph.D. thesis, University of Illinois at Chicago, Chicago, IL, 1996.
- [15] A. GOETZ, *Perturbation of 8-attractors and births of satellite systems*, Internat. J. Bifur. Chaos Appl. Sci. Engrg., 8 (1998), pp. 1937–1956.
- [16] A. GOETZ, *Dynamics of a piecewise rotation*, Continuous and Discrete Dynamical Systems, 4 (1998), pp. 593–608.
- [17] A. GOETZ, *Stability of piecewise rotations and affine maps*, Nonlinearity, 14 (2001), pp. 205–219.
- [18] A. GOETZ, *Dynamics of a piecewise isometries*, Illinois J. Math., 44 (2000), pp. 465–478.
- [19] A. GOETZ, *A self-similar example of a piecewise isometric attractor*, in Dynamical Systems (Luminy-Marseille, 1998), World Sci. Publishing, River Edge, NJ, 2000, pp. 248–258.
- [20] B. KAHNG, *Dynamics of symplectic piecewise affine elliptic rotation maps on tori*, Ergodic. Theory Dynam. Systems, 22 (2002), pp. 485–505.
- [21] A. KATOK AND B. HASSELBLATT, *Introduction to the Modern Theory of Dynamical Systems*, Cambridge University Press, Cambridge, UK, 1995.

- [22] H. B. KEYNES AND D. NEWTON, *A “minimal”, non-uniquely ergodic interval exchange transformation*, Math. Z., 148 (1976), pp. 101–105.
- [23] J. C. LAGARIAS AND E. RAINS, *Dynamics of a Family of Piecewise-Linear Area-Preserving Plane Maps I, Invariant Circles*, preprint, arXiv:math.DS/031294v1, 2003.
- [24] R. S. MACKAY AND J. MEISS, *Hamiltonian Dynamical Systems: A Reprint Selection*, Adam Hilger Press, Bristol, UK, 1987.
- [25] H. MASUR, *Hausdorff dimension of sets of nonergodic foliations of a quadratic differential*, Duke Math. J., 66 (1992), pp. 387–442.
- [26] H. MASUR AND J. SMILLIE, *Hausdorff dimension of sets of nonergodic measured foliations*, Ann. of Math. (2), 134 (1991), pp. 455–543.
- [27] A. J. SCOTT, C. A. HOLMES, AND G. MILBURN, *Hamiltonian mappings and circle packing phase spaces*, Phys. D, 155 (2001), pp. 34–50.
- [28] A. J. SCOTT, *Hamiltonian mappings and circle packing phase spaces: Numerical investigations*, Phys. D, 181 (2003), pp. 45–52.
- [29] W. A. VEECH, *Strict ergodicity in zero dimensional dynamical systems and the Kronecker-Weyl theorem mod 2*, Trans. Amer. Math. Soc., 140 (1969), pp. 1–34.
- [30] F. VIVALDI AND I. VLADIMIROV, *Pseudo-randomness of round-off errors in discretized linear maps on the plane*, Internat. J. Bifur. Chaos Appl. Sci. Engrg., 13 (2003), pp. 3373–3393.
- [31] M. WOJTKOWSKI, *A model problem with the coexistence of stochastic and integrable behaviour*, Comm. Math. Phys., 80 (1981), pp. 453–464.